AFRL-AFOSR-VA-TR-2024-0043

Addressable Surface-Curvature Driven Mesa Top Single Quantum Dot Based Single Photon Source Array Integrated On-Chip with Dielectric Light Manipulating Elements

Madhukar, Anupam
UNIVERSITY OF SOUTHERN CALIFORNIA
3720 S FLOWER ST
FL 3
LOS ANGELES, CA, 90089
USA

11/30/2023
Final Technical Report

Air Force Research Laboratory
Air Force Office of Scientific Research
Arlington, Virginia 22203
Air Force Materiel Command

REPORT DOCUMENTATION PAGE

PLEASE DO NOT RETURN YOUR FORM TO THE ABOVE ORGANIZATION.

1. REPORT DATE	2. REPORT TYPE	3. DATES COVERED	
20231130	Final	START DATE 20170915	END DATE 20221231

4. TITLE AND SUBTITLE
Addressable Surface-Curvature Driven Mesa Top Single Quantum Dot Based Single Photon Source Array Integrated On-Chip with Dielectric Light Manipulating Elements

5a. CONTRACT NUMBER	5b. GRANT NUMBER	5c. PROGRAM ELEMENT NUMBER
	FA9550-17-1-0353	61102F
5d. PROJECT NUMBER	**5e. TASK NUMBER**	**5f. WORK UNIT NUMBER**

6. AUTHOR(S)
Anupam Madhukar

7. PERFORMING ORGANIZATION NAME(S) AND ADDRESS(ES)
UNIVERSITY OF SOUTHERN CALIFORNIA
3720 S FLOWER ST
FL 3
LOS ANGELES, CA 90089
USA

8. PERFORMING ORGANIZATION REPORT NUMBER

9. SPONSORING/MONITORING AGENCY NAME(S) AND ADDRESS(ES)
Air Force Office of Scientific Research
875 N. Randolph St. Room 3112
Arlington, VA 22203

10. SPONSOR/MONITOR'S ACRONYM(S)
AFRL/AFOSR RTB1

11. SPONSOR/MONITOR'S REPORT NUMBER(S)
AFRL-AFOSR-VA-TR-2024-0043

12. DISTRIBUTION/AVAILABILITY STATEMENT
A Distribution Unlimited: PB Public Release

13. SUPPLEMENTARY NOTES

14. ABSTRACT
This Final Technical Report briefly captures the highlights of the accomplishments under grant number FA9550-17-1-0353 (Program Manager Dr. Gernot Pomrenke) whose basic goal was to explore the potential of our new class of spatially ordered arrays of single quantum dots (SQD) dubbed mesa-top single quantum dot (MTSQD) as on-demand single photon sources (SPS). Spatially-ordered arrays of quantum emitters are the essential, but hitherto missing, component for the long-sought platform for fabricating on-chip integrated quantum optical circuits. During this period (Sept.15, 2017 – Dec. 31, 2022), despite the unanticipated delays and disruptions due the COVID-19 induced shutdowns from March 2020 to July 2021, we successfully reached several major milestones critical to realizing quantum optical circuits. The driving vision, goals set for this grant, and accomplishments are captured in this final technical report, as are some comments on the continuing efforts. The advances made under this grant have brought the field one essential step closer to realizing on-chip scalable quantum photonic systems.

15. SUBJECT TERMS

16. SECURITY CLASSIFICATION OF:			17. LIMITATION OF ABSTRACT	18. NUMBER OF PAGES
a. REPORT	b. ABSTRACT	c. THIS PAGE		
U	U	U	UU	21

19a. NAME OF RESPONSIBLE PERSON	19b. PHONE NUMBER *(Include area code)*
GERNOT POMRENKE	426-8426

Standard Form 298 (Rev.5/2020)
Prescribed by ANSI Std. Z39.18

Final Technical Report

Grant No. AFOSR FA9550-17-1-0353

Period: Sept. 15, 2017 to December. 31, 2022

Addressable Surface-Curvature Driven Mesa Top Single Quantum Dot Based Single Photon Source Array Integrated On-Chip with Dielectric Light Manipulating Elements

Program Manager: Dr. Gernot Pomrenke (AFOSR)

Air Force Office of Scientific Research/NE
875 North Randolph Street, Arlington, VA 22203

PI: Dr. Anupam Madhukar
University of Southern California
Los Angeles, CA 90089-0241
Tel. (213) 740-4325
e-mail: madhukar@usc.edu

This Final Technical Report briefly captures the highlights of the accomplishments under grant number FA9550-17-1-0353 (Program Manager Dr. Gernot Pomrenke) whose basic goal was to explore the potential of our new class of *spatially ordered arrays* of single quantum dots (SQD) dubbed mesa-top single quantum dot (MTSQD) as *on-demand single photon sources* (SPS). Spatially-ordered arrays of quantum emitters are the essential, but hitherto missing, component for the long-sought platform for fabricating on-chip integrated quantum optical circuits. During this period (Sept.15, 2017 – Dec. 31, 2022), despite the unanticipated delays and disruptions due the COVID-19 induced shutdowns from March 2020 to July 2021, we successfully reached several major milestones critical to realizing quantum optical circuits. The driving vision, goals set for this grant, and accomplishments are captured in this final technical report, as are some comments on the continuing efforts. The advances made under this grant have brought the field one essential step closer to realizing on-chip scalable quantum photonic systems.

Outline

I. Vision and Objectives

Figure 1 captures our vision for an on-chip minimal quantum photonic subsystem that embodies the basic functional elements needed to achieve controlled interference and entanglement of photons from distinct but known single (or pairs of) photon sources to construct the basic resource for quantum information processing (QIP)—clusters of entangled photon / matter qubit states.

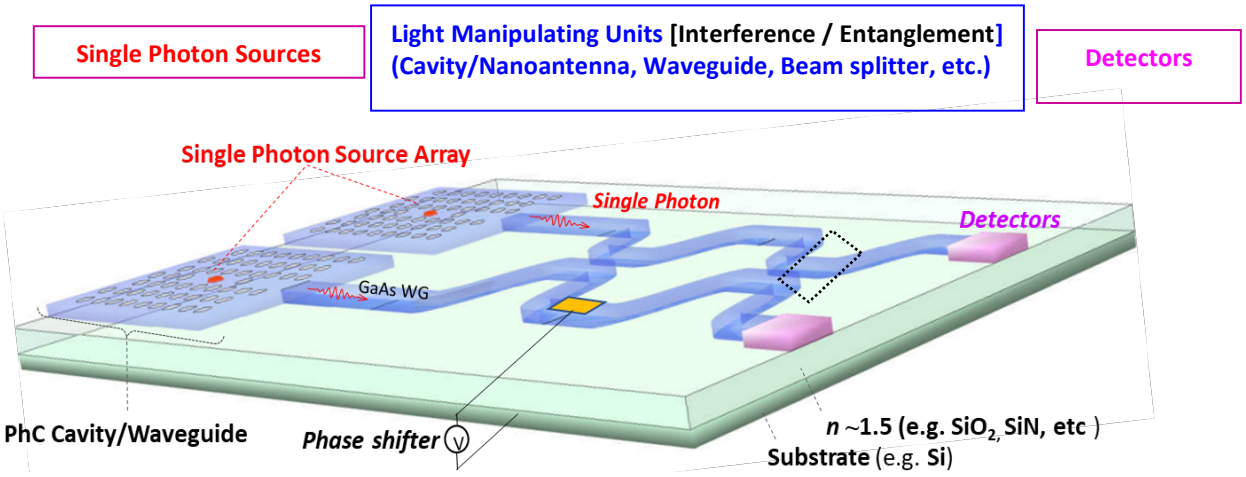

Fig.1 Schematic of a minimal on-chip quantum photonic system that captures the essential elements of the controlled generation of entangled photon qubit – matter qubit building block underlying scalable QIP photonic networks. [Adapted from ref.1]

To date several demonstrations of integration of one or more elements of the system depicted schematically in Fig.1[adapted from ref.1] have been reported but are limited to one or two sources as they are largely built around *SPS chosen from a random distribution in space and spectral emission* [2,3]. The basic **objective of the program** undertaken-- **whose findings are summarized here--** was **to realize SPSs in the *required spatially-ordered* designed arrays with emitted *photon characteristics* across the array *above the threshold requirements for their use in networks*** for quantum communication, computing, metrology / sensing, and simulations of fundamental material behavior. These **requirements** on the SPS ***are captured in Fig.2*** taken from our recent publication [1] supported by this grant. Figure 2 captures the fact that semiconductor quantum dots are, to-date, the only *demonstrated* solid-state on-chip *bright* sources that provide, *on-demand*, single and entangled pairs of photons with spectral characteristics meeting the requirements of purity and visibility for linear optical quantum computing and quantum-limit sensing / imaging. Prior to our introduction [4] and development [5,6,7] of the novel spatially-ordered MTSQDs (mesa-top single quantum dots) in designed arrays, and since, the epitaxial quantum dots employed in the literature to demonstrate these characteristics as proof-or-principle are opportunistically chosen from uncontrolled distributions of SQDs—the so-called self-assembled quantum dots (SAQDs) that form spontaneously (thus uncontrolled) at random locations and times, thus giving SQDs of varying size, composition and shapes resulting in highly inhomogeneous (typically ~40nm) spectral emission width [3]. This deficiency prevents such SQDs from providing a basis for scalable technological platforms and

has, regrettably, led to attention moving away from "quantum dots" as viable quantum emitters for on-chip QIP technologies.

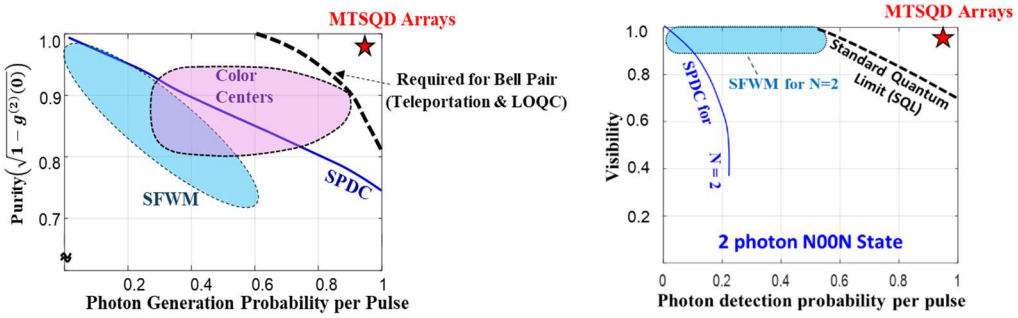

Fig.2 Shows the required performance regime (above the broken lines) for a single photon source to serve quantum information processing platforms [from ref. 1]: (a) purity versus photon generation probability per pulse for linear optical quantum computing; (b) visibility versus photon detection probability per pulse for 2-photon NOON state generation for quantum sensing at the standard quantum limit. Semiconductor epitaxial quantum dots are the only solid-state quantum emitters that *individually* have been demonstrated to meet these criteria. [From Ref.1]

Our contribution under this grant is the ***realization of spatially-ordered arrays* of SDQs as quantum emitters** *with emission wavelength nonuniformity that is within demonstrated local "on-resonance" tuning technologies* ***while maintaining their spectral characteristics as demanded by Fig.2.*** *Thus, exploration of a viable path to fabrication of scalable on-chip quantum photonic circuits / networks is enabled for the first time.*

II. List of Scientific Milestones Accomplished

(1) Established the mesa top single quantum dots (MTSQDs) in spatially-regular arrays as highly efficient (nearly 100%) single photon source (SPS) array with as low as <1.8nm emission nonuniformity and single photon emission purity >99.5% [Ref. 6]

(2) Established a protocol for planarizing the *as-grown nonplanar pyramidal morphology* of the MTSQD SPS array, necessary for subsequent fabrication of optical circuits / networks of interconnected SPSs. [Ref.6]

(3) Demonstrated the long-sought platform of an array of *planarized* $In_{0.5}Ga_{0.5}As$ MTSQDs exhibiting single photon emission purity >98% and nonuniformity <4nm across 50X50 arrays of 2500 MTSQDs distributed over ~1Cm radius. [Ref.8]

(4) Utilizing STEM (scanning transmission electron microscopy), established growth profile evolution for different as-etched mesa morphologies, their effect on mesa top SQD formation, and subsequent planarization of the MTSQD pyramidal morphology. [ref. 1]

(5) Revealed for the first time the structural (size and shape) nature and uniformity of InGaAs MTSQDs in the array and their location with an accuracy of ~5nm. Laterally and ~1nm vertically. [Ref. 9]

(6) Established instrumentation for resonant excitation and two-photon interference (TPI) measurements in the Hong-Ou-Mandel (HOM) configuration to examine the visibility of photons from the buried planarized MTSQD arrays. [Ref.1]

(7) Demonstrated that the photon indistinguishability from MTSQDs *without a resonant cavity* is ~82% at 11.5K (limited by the measurement temperature), extrapolated to reach greater than 95% at ~4K. [Ref.1]

(8) Scaled individual array size to 50 X 50 over 250μmX250μm with such arrays distributed over 1Cm radius. [Ref.8]

(9) Established instrumentation for large-area *spatially-resolved* optical imaging and demonstrated bright emission from large 50 X 50 MTSQD arrays. [Ref.10]

(10) Established the design of MTSQDs in a cavity structure for the measurement and testing of near-unity indistinguishability of photons emitted from the MTSQDs.

These achievements provide further evidence of the uniqueness and exceptionality of MTSQDs as a suitable platform for the fabrication of scalable MTSQD-light manipulating units (cavity, waveguide, etc.) interconnected to provide quantum optical circuits.

III. Programmatic Accomplishments: Publications, Presentations, Personnel Supported

(a) **Publications** (In peer-reviewed journals)

1. Jiefei Zhang, Swarnabha Chattaraj, Siyuan Lu and Anupam Madhukar, "Highly pure single photon emission from spectrally uniform surface-curvature directed mesa top single quantum dot ordered arrays", **Appl. Phys. Lett. 114**, 071102, **(2019)** https://doi.org/10.1063/1.5080746
2. S. Chattaraj, J. Zhang, S. Lu, and A. Madhukar, "On-Chip Integrated Single Photon Source Optically Resonant Metastructure Based Scalable Quantum Optical Circuits", **IEEE Jour. Quantum Electronics**, **56**, 1, 9300109 **(2020)** https://doi.org/10.1109/JQE.2019.2952387
3. J. Zhang, Q. Huang, S. Chattaraj, L. Jordao, S. Lu, and A. Madhukar, "Buried spatially-regular arrays of spectrally uniform single quantum dots as on-chip scalable single photon sources for quantum optical circuits", **APL Photonics**, **5**, **116106 (2020)** https://doi.org/10.1063/5.0018422
4. J. Zhang, Q. Huang, S. Chattaraj, L. Jordao, S. Lu, and A. Madhukar, "On-chip scalable highly pure and indistinguishable single-photon sources in ordered arrays: Path to quantum optical circuits" **Science Advances**, **8, eabn2 (2022)** https://doi.org/10.1126/sciadv.abn9252

(b) **Publications** (Unreviewd)

5. 1. J. Zhang, S. Chattaraj, Q. Huang, L. Jordao, S. Lu and A. Madhukar, "Indistinguishable single photons from spatially-ordered array of highly efficient and pure mesa-top single quantum dots: A step closer to on-chip quantum optical

circuits", **arXiv: 2108.01428v2** (2021)
https://doi.org/10.48550/arXiv.2108.01428

(c) Presentations

i. Presentations at meetings, but not published in Conference Proceedings

2022

1. **(Invited Talk)** Jiefei Zhang, Q. Huang, S. Chattaraj, L. Jordao, S. Lu and A. Madhukar, "A New platform of single photon source arrays for on-chip quantum photonic", **IEEE Research and Applications of Photonics in Defense Conference, Sept. 2022**
2. **(Contributed Talk)** Q. Huang, J. Zhang, S. Chattaraj, L. Jordao, S. Lu and A. Madhukar, "Highly Uniform and Indistinguishable Scalable Single Photon Source Arrays—Towards Quantum Optical Circuits". **MRS 2022 Fall Meeting. Session EQ03.14.03**
3. **(Poster presentation)** L. Jordao, J. Zhang, Q. Huang, S. Chattaraj, S. Lu and A. Madhukar, "Bright and Highly Uniform, Pure, Indistinguishable, Spatially-Ordered Single Quantum Dot Emitters—Molecular Beam Epitaxial Growth and Structural Characterization". **MRS Fall 2022 Meeting. Session EQ03.18.16**

2021

2**. (Invited Talk)** Anupam Madhukar, Jiefei Zhang, Qi Huang, Swarnabha Chattaraj, Lucas Jordao, and Siyuan Lu, "Single Photon Emitter Arrays for On-chip Quantum Photonics", Invited talk in Session "Semiconductor Materials and Quantum Nanoscience", WB2.1, **IEEE Research and Applications of Photonics in Defense Conference, Aug 2021.**

3. J. Zhang, Qi Huang, Lucas Jordao, Swarnabha Chattaraj, Siyuan Lu, Anupam Madhukar, "A New Paradigm for On-chip Quantum Photonics: Highly Uniform Single Photon Source Arrays", TuA2.3, Oral Presentation in Session "Nonlinear Effects and Quantum New Devices", **IEEE Photonics Conference, Oct 2021.**

4. Swarnabha Chattaraj, Jiefei Zhang, Siyuan Lu, and Anupam Madhukar, "Mie Resonance Based Quantum Optical Circuits Integrated with on-chip Single Photon Source Array for Quantum Information Processing", *Oral Presentation* in Session "Integrated Quantum Photonics", TuA4.3, **IEEE Research and Applications of Photonics in Defense Conference, Aug 2021.**

5. Jiefei Zhang, Qi Huang, Lucas Jordao, Swarnabha Chattaraj, Siyuan Lu, Anupam Madhukar, "Planarized Ordered Uniform Mesa-top Single Quantum Dot Single Photon Source Arrays: A Platform for Scalable Quantum Optical Networks", *Oral Presentation* in Session "Hybrid Photonic Systems", B31.13, **APS March Meeting, March 2021**.

6. Swarnabha Chattaraj, Jiefei Zhang, Siyuan Lu, Anupam Madhukar, "Entanglement in optical circuits based on Mie resonant metastructures integrated with on-chip array of single photon sources", *Oral Presentation* in Session "Hybrid Photonic Systems", B31.11, **APS March Meeting, March 2021.**

2020

7. S. Chattaraj, J. Zhang, S. Lu and A. Madhukar, "Mie Resonant Dielectric Metastructure based Quantum Optical Circuits Integrated with Single

Photon Source: A new paradigm for Quantum Information Processing", **G65.00013,** Oral Presentation, **APS March Meeting, Denver, Colorado. Mar. 2020.**

8. J. Zhang, S. Chattaraj, S. Lu and A. Madhukar, "On-chip Integrable Highly Spectrally Uniform Ordered Semiconductor Quantum Dot Single Photon Source Arrays for Scalable Quantum Optical Networks", **J65.00002**, Oral Presentation, **APS March Meeting, Denver, Colorado. Mar. 2020.**
9. **(Invited)** A. Madhukar, J. Zhang, S. Chattaraj, and S. Lu, "A New Paradigm for Scalable Quantum Optical Circuits: On-Chip Single Photon Source Arrays Integrated with Optically Resonant Metastructure Based Light Manipulating Units", **MRS Spring Meeting Phoenix, Arizona, April. 2020**.
10. **(Invited Talk)** J. Zhang, S. Chattaraj, Q. Huang, L. Jordao, S. Lu and A. Madhukar, "Mesa-Top Single Quantum Dot Arrays as Single Photon Sources: A new paradigm for On-chip Quantum Photonics", **Asia Communications and Photonics Conference (ACPC) 2020**, China (October, 2020)
11. **(Invited Talk)** Anupam Madhukar, Jiefei Zhang, Swarnabha Chattaraj, and Siyuan Lu, "A New Paradigm for Scalable Quantum Optical Circuits—On-Chip Single Photon Source Arrays Integrated with Optically Resonant Metastructure Based Light Manipulating Units", Invited Talk in Session "Single Photon Emitters", S.EL06.05.02, **MRS Spring/Fall Meeting, Nov 29-Dec 4, 2020.**
12. Swarnabha Chattaraj, Jiefei Zhang, Siyuan Lu, Anupam Madhukar, "Mie Resonant Dielectric Metastructure based Optical Circuits Integrated with Quantum Dot Single Photon Source for on-chip Scalable Quantum Information Processing", *Oral Presentation* in Symposium "Photonic Materials for information Processing and Computing**" MRS Spring/Fall Meeting, Nov 29-Dec 4, 2020.**

2019

13. Swarnabha Chattaraj, Jiefei Zhang, Siyuan Lu and Anupam Madhukar, "Integrated Quantum Networks of Mie-resonance based All-Dielectric Optical Circuits with Single Photon Sources for Quantum Entanglement", **P29.7**, Oral Presentation in the Symposium on "Semiconductor QD Architectures and Quantum Photonics" in the **APS March Meeting Boston, Massachusetts. Mar. 2019.**
14. Jiefei Zhang, Swarnabha Chattaraj, Siyuan Lu and Anupam Madhukar, "On-chip Integrable Spectrally Uniform Ordered Quantum Dot Single Photon Source Array with High Emission Purity (>98.99%) for Scalable Quantum Optical Networks", **P29.5**, Oral Presentation in the Symposium on "Semiconductor QD Architectures and Quantum Photonics" in the **APS March Meeting Boston, Massachusetts. Mar. 2019.**
15. **(Invited)** Jiefei Zhang, Siyuan Lu, Swarnabha Chattaraj and Anupam Madhukar, "On-Chip Integrated Scalable Single Photon Source-All-Dielectric Metastructure Based Nanophotonic Quantum Optical Circuits",

Oral Presentation in the Session "Quantum Device" in the **2019 China Quantum Information Science and Technology Symposium, Ji'nan, China, May 2019**.

16. **(Invited)** Jiefei Zhang, Siyuan Lu, Swarnabha Chattaraj and Anupam Madhukar, "On-Chip Integrated Scalable Single Photon Source-All Dielectric Metastructure Based Nanophotonic Quantum Optical Circuits towards Quantum Information Science", Oral Presentation, **South Bay Interdisciplinary Science Center & IOP CAS Young Scientists Symposium, Dongguan, China, May 2019.**
17. **(Invited)** Anupam Madhukar, Jiefei Zhang, Swarnabha Chattaraj, Siyuan Lu, "On-Chip Integrated Scalable Single Photon Source-Optically Resonant Metastructure Based Quantum Optical Circuits: A new paradigm for quantum information processing", **C2-07**, Oral Presentation in Symposium C: Semiconductor Photonics, **International Conference on Materials for Advanced Technology, Singapore, June, 2019.**
18. Swarnabha Chattaraj, Jiefei Zhang, Siyuan Lu, Anupam Madhukar, "On-chip Scalable Integrated Quantum Photonic Networks based on Quantum Dot Single Photon Source Array Integrated with Dielectric Light Manipulating Circuits", **WF1.4**, Oral Presentation in Symposium on "Valleytronics and Single and Entangled Photons" in **IEEE Summer Topical Meeting, Fort Lauderdale, Florida, July, 2019**

Honors and Awards

Best Paper, Lucas Jordao et al., MRS Fall 2022 Meeting, Session EQ03.18.16.
Invited Talk, IEEE-RAPID 2022, Sept.12-14,, 2022; J. Zhang,
Invited Talk, IEEE-RAPID 2021, Aug. 2-4, 2021; A. Madhukar and J. Zhang,
Invited Talk, MRS Spring/Fall Meeting, Nov. 29 - Dec.4, 2020; A. Madhukar and J. Zhang,
Invited Talk, ACPC, Oct 2020, J. Zhang,
Invited Talk, International Conference on Materials for Advanced Technology, Singapore, June, 2019; A. Madhukar, J. Zhang, S. Chattaraj
Invited Talk, China Quantum Information Science and Technology Symposium, Ji'nan, China, May 2019; Jiefei Zhang
Invited Talk, South Bay Interdisciplinary Science Center & IOP CAS Young Scientists Symposium, Dongguan, China, May 2019; Jiefei Zhang

Title of Patents Disclosed during the reporting period

"On-Chip Integrable Ordered and Highly Spectrally Uniform Single Photon Sources for Scalable Quantum Optical Circuits"

Patents Awarded during the reporting period

None

Student/Supported Personnel Metrics

(a) Number of Undergraduate STEM Students

Three.
Olivia Brasher (EE), Emily Kretschmer (Chem. Eng.), Larry Li (Physics).

(b) Number of Graduate STEM Students
Three
Swarnabha Chattaraj, Qi Huang and Lucas Jordao

(c) Number of Students that received a STEM degree
One.
Swarnabha Chattaraj [PhD in EE]

(d) Other Research staff
Postdoctoral Fellow: Dr. Jiefei Zhang 2018-2020
Research Asst. Professor: Dr. Jiefei Zhang 2020-2021

Technology transfer

None

IV. Description of Major Accomplishments

The accomplishments under this grant build upon our ground-breaking demonstration [4,5] of spatially-ordered arrays of GaAs(001)/$In_{0.5}Ga_{0.5}As$/GaAs mesa-top single quantum dots (MTSQDs) as highly pure (~99.5%) single photon sources with unprecedented spectral uniformity standard deviation of ~4nm across 5X8 arrays of 40 MTSQDs distributed over ~1000μm^2. The ~4nm nonuniformity is limited by the alloy concentration fluctuation and disorder scattering across the array. The challenge under this grant was thus to next examine (1) the emitted two photon HOM *indistinguishability* necessary to assess the potential usefulness of these quantum emitters, (2) to find a fabrication protocol that would seamlessly during growth convert the pyramidal morphology of the as-grown MTSQD into a planarized surface across the wafer—a requirement for being able to fabricate interconnected network of quantum emitters for quantum information processing, and (3) demonstrate scaling of the arrays from 5X8 to large sizes containing ~100,000 to 1000,000 MTSQDs over areas ~1Cm^2.

The following captures the chronological development of the efforts that have led to the first platform of scalable spatially-ordered on-demand single quantum emitters in four conceptual and implementation stages: (i) demonstration of reproducible ordered epitaxial single quantum dots on the top of growth-controlled as-patterned size-reduced nanomesas in designed arrays and their single photon characteristics; (ii) development of protocol for the planarization of the pyramidal morphology of the as-synthesized MTSQDs while maintaining single photon emission characteristics; (iii) scalability to large arrays and areas.

IV.1 As-Synthesized Pyramidal (Un-planarized) MTSDQ Arrays: The Starting Point

Going beyond the alloy quantum dots that suffer from inherent alloy fluctuation-induced spectral nonuniformity, we examined [6] binary GaAs/InAs/GaAs MTSQDs. Figure 3 summarizes the findings. Fig. 3(a) shows SEM images of the typical starting nanomesa, the shape and morphology after the growth of the InAs SQD residing near the pyramidal mesa apex, and a partial view of the 5X8 array. An unprecedented spectral uniformity of 1.8nm over 1000um^2 is seen in the emission wavelength display of Fig. 3(b) and histogram of Fig.3(c). This is a factor of ~20 narrower as compared to the most popularly employed self-assembled island quantum dots (SAQDs) [3]. The observed unprecedented uniformity of ~1.8nm across the binary

InAs MTSQD array is achieved by eliminating the fluctuation of indium concentration amongst the $In_{0.5}Ga_{0.5}As$ alloy MTSQDs which, as we showed earlier, give ~6nm nonuniformity.

It is important to note that, *strikingly*, in this highly uniform SQD array, ***there are (i) 49 pairs of SQDs (marked by like-color circles in Fig. 3(b)) emitting within 0.2nm (280μeV) and (ii) clusters of up to 6 QDs emitting within 0.2nm (280μeV).*** These SQDs can be brought in resonance with each other with current on-chip turning technology using Stark effect or local heating *to realize photon interference and entanglement between photons emitted from distinct but known (chosen) SQDs*. Realizing this has been the long elusive goal that has prevented good demonstrations of quantum optics effects from being converted into quantum optical technology.

The above-noted findings for the MTSQDs in arrays testify to their considerable promise for demonstrating controlled generation of hierarchical entanglement of increasing number of photons, i.e., the so-called **cluster states**, that are the **essential quantum resource** underpinning optical quantum technologies sought for LOQC (linear optical quantum computing), secure communication, and quantum-limit sensing and metrology. The MTSQDs, potentially hybrid integrated with silicon photonics, offer the best potential for realizing **scalable** on-chip quantum optical circuits as visualized in Fig.1.

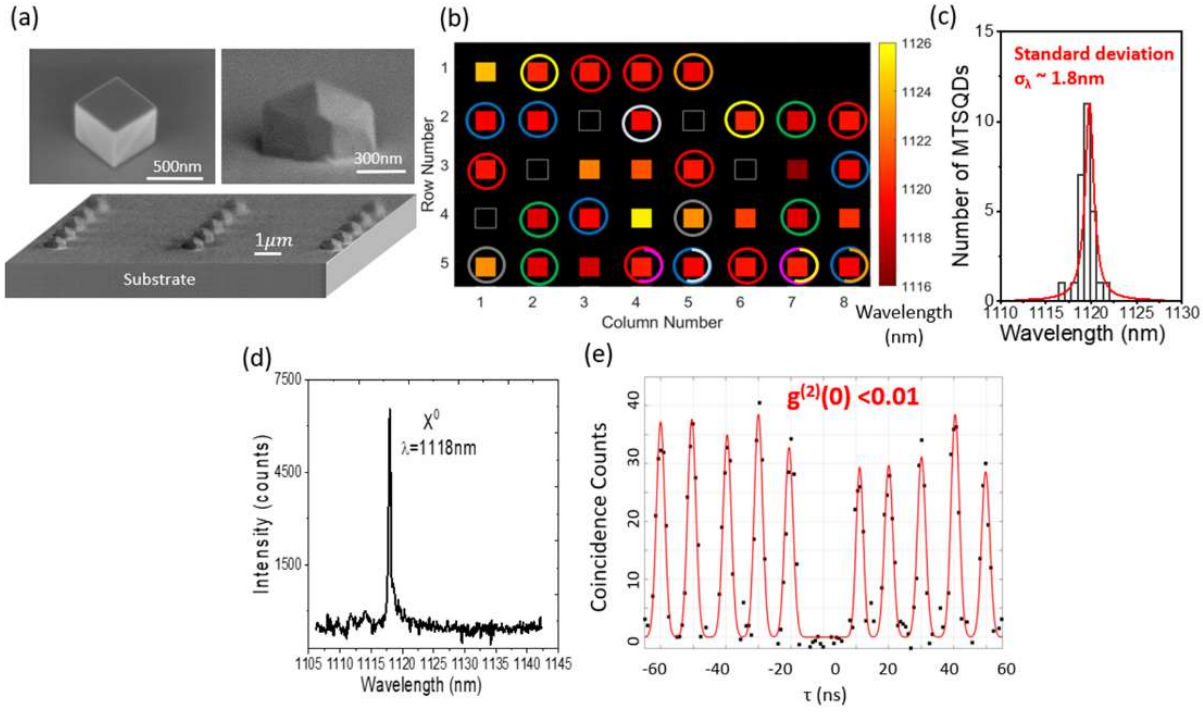

Fig.3. (a) SEM image showing a part of a 5×8 array of binary GaAs/InAs/GaAs MTSQD single photon sources (SPSs) grown on mesas with vertical side walls (SEM, upper left). A magnified SEM of a single mesa bearing MTSQD is shown in upper right SEM image. (b) The measured photoluminescence peak wavelength of each MTSQD in the array shown as color coded blocks. The black blocks with white outline indicate non-emitting MTSQD pixels. Like-color circles marks the MTSQDs that are emitting within 0.2nm of each other. (c) Histogram showing the emission wavelengths of the array are centered at 1120nm with an unprecedented 1.8nm standard deviation. (d) Photoluminescence from a representative InAs MTSQD in the 5×8 array measured at 18K showing exciton emission at 1118nm with instrument limited linewidth of 0.2nm (280ueV). (e) Corresponding histogram of coincidence counts measured showing $g^{(2)}(0) < 0.01$ and thus single photon purity >99.5%. [From ref.6]

The use of InAs also shifts the wavelength by nearly 200nm to longer values ~1120nm. A typical PL from an InAs MTSQD in the array is shown in Fig. 3(d) with emission at 1118nm and an instrument limited linewidth of 0.2nm (280μeV). These binary InAs MTSQDs show a $g^{(2)}(0) < 0.01$—indicating single photon emission purity greater than 99.5% (Fig. 3(e)) [4]. By further tuning the size and shape of the as-grown MTSQDs, one can realize such ordered and spectrally uniform SPS arrays with wavelengths up to communication wavelength around 1550nm.

IV.2 Planarization of the Pyramidal MTSQD Morphology

While Fig.3 captures the first demonstration of on-chip *and* on-demand single photon emitters in spatially-ordered arrays with unprecedented spectral emission uniformity and single photon purity, the pyramidal morphology at the stage of the MTSQD formation (panel a) is unsuited to their use in on-chip optical networks / circuits which demand fabrication of a variety of emitted-photon manipulation elements (e.g. cavity, waveguide, beam couplers, phase shifters, etc.) to ensure controlled interference and entanglement between the desired photons required by on-chip quantum optical circuits. Thus, planarizing the pyramidal morphology of the MTSQDs is the next step towards enabling evaluation of their suitability for on-chip quantum optical circuits. Below, we summarize our achievement of this objective.

Planarization of the morphology during continued growth following the formation of the MTSQD (referred to here as the planarizing overlayer) requires the reversal of the interfacet migration direction and incorporation rate of the atoms arriving from the vapor flux on the nonplanar growth front. This is effectively the opposite of what led to the size-reducing epitaxy and thus the formation of the quantum dot on the mesa-top in the first place. While the MTSQDs of Fig.3 were grown on nanomesas with vertical sidewalls as seen in Fig.3(a), reversing the stress-gradient driven atom migration to achieve faster incorporation in the valley regions requires a mesa shape as shown in Fig.4(a) that we call pedestal base. On such a shape, growth following the formation of the MTSQD and mesa-top pinch-off results in the morphology shown by the SEM images in panels (b) to (d). The corresponding AFM images are shown in panels (d) to (f). The various stages of planarization for the same amount of overlayer material delivered (~210nm) under identical growth conditions are evident.

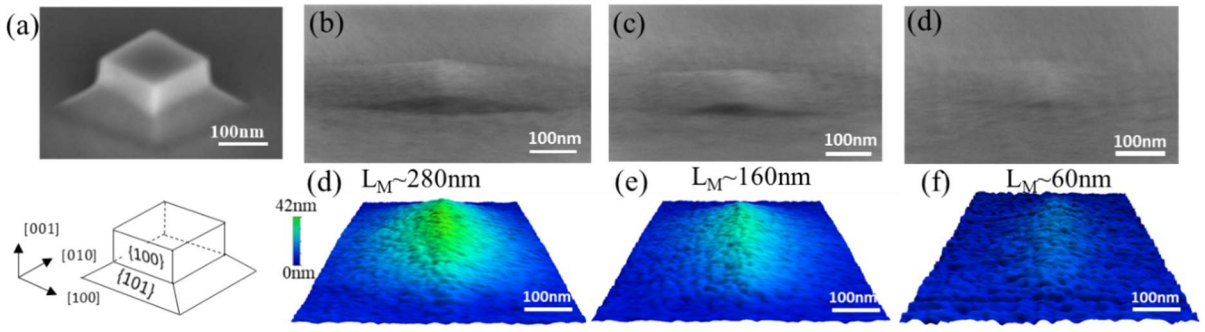

Fig. 4. For growth on mesas with pedestal (panel a, SEM image of a mesa with lateral size LM~160nm and a schematic), shown are SEM (panels b, c, and d) and corresponding AFM (panels d, e and f) images of the surface morphology after the growth of ~210nm of a morphology planarization GaAs overlayer. The three SEM and AFM images correspond to starting <100> edge oriented mesas of lateral sizes LM ~280nm, ~160nm, and ~60nm with the vertical{100}sidewalls of depth 65nm and {101}pedestal base facets of equivalent depth 65nm.[From ref.6]

Although our demonstration that a pedestal-shaped mesa enables planarization of the pyramidal morphology of the MTSQD which is essential for the use of the buried SQD arrays for subsequently fabricating quantum optical circuits, it is equally essential that one has control on growth to reproduce the shape, size, and location of the quantum dots across the array and from growth to growth. To this end we undertook STEM (scanning transmission electron microscope) based studies of structural and chemical aspects of the notion of quantum dots as discussed next.

IV.3 Structural Studies: Surface Profile Evolution with Growth and MTSQD Location

The STEM based structural studies comprise three aspects:

(i) the evolution of the growth front profile from that of the as-patterned mesa

(ii) the shape and size (base and height) of the formed single quantum dot

(iii) the lateral and vertical location of the single quantum dot on mesa top

Of course, the above noted characteristics are needed for statistically significant number of SQDs of the arrays to establish the degree of structural and composition uniformity that in turn controls the uniformity of the all-important optical characteristics.

Figure 5 shows high magnification two-beam Z-contrast images of three consecutive buried MTSQDs in an array. While the default grey colored regions represent GaAs, the dark lines are AlAs marker layers introduced to reveal the starting profiles of nanomesas and their evolution as the growth proceeds. Note the expected size-reduction and the absence of the AlAs dark lines from the mesa sidewalls until after the pinch-off indicating the lack of cation incorporation on the mesa sidewalls until mesatop pinch-off. Note the planarization of the evolving growth front seen following the pinch-off. The white line represents the deposited InGaAs 4.25ML that deposits as flat thin *quantum well* in the valley regions between the mesas and on the size-reduced (to ~20nm) mesa top to form the region (white) of the single quantum dot. This is shown magnified in the high-resolution STEM images in Fig. 6. Note the accurate location of the QD.

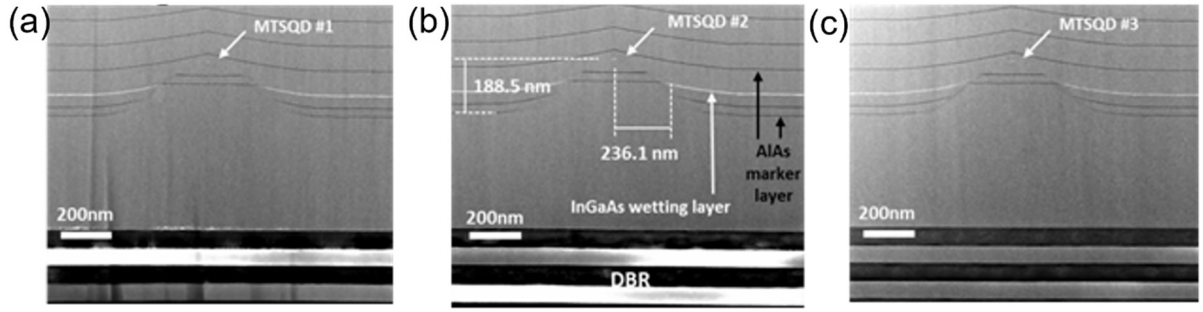

Fig 5. Panels (a) – (c) show high- magnification (x1.2M) STEM images of the three MTSQD regions revealing the evolution of the growth front profile (dark lines) to mesa-top pinch-off, followed by planarization owing to the pedestal-shape of the as-patterned nanomesas. Note the accurate positioning of the quantum dot (white regions).

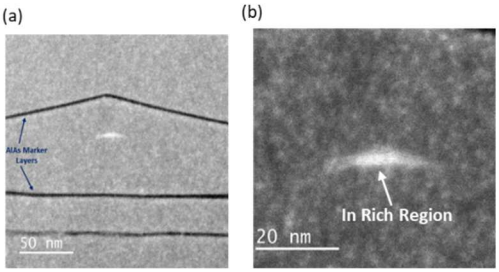

Fig.6 (a) High-angle annular dark field (HAADF) image of the mesa-top region showing the InGaAs SQD as the white region (b) A magnified view of the region (white) of the InGaAs single quantum dot buried in GaAs (grey). [Ref.1]. See Fig.7 also.

IV.4 The MTSQD Chemical Composition Distribution

The employed STEM also has energy dispersive spectroscopy (EDS) to reveal elemental spatial distribution. Fig.7 below captures the distribution of In (violet), Ga (blue) and Al (green), confirming the size-reduction during initial GaAs growth leading to the desired mesa-top size ~20nm for the deposition of the 4.25ML InGaAs to form the SQD on the mesa top while in the valley regions only quantum well form owing to the deposition amount chosen strategically to be below the critical value for the self-assembled island quantum dot formation in the planar valley regions. The *lateral placement of the QDs is accurate to within 5nm and the vertical placement to within ~1nm*, both controlled by the *as-patterned* mesa lateral size and depth distributions. To reduce these ranges, needed are efforts on developing etching protocols that ensure improved control on the shape, lateral size, and depth of as-etched mesas across wafer size (such as already developed for nanoimprint lithograph of silicon nanomesas).

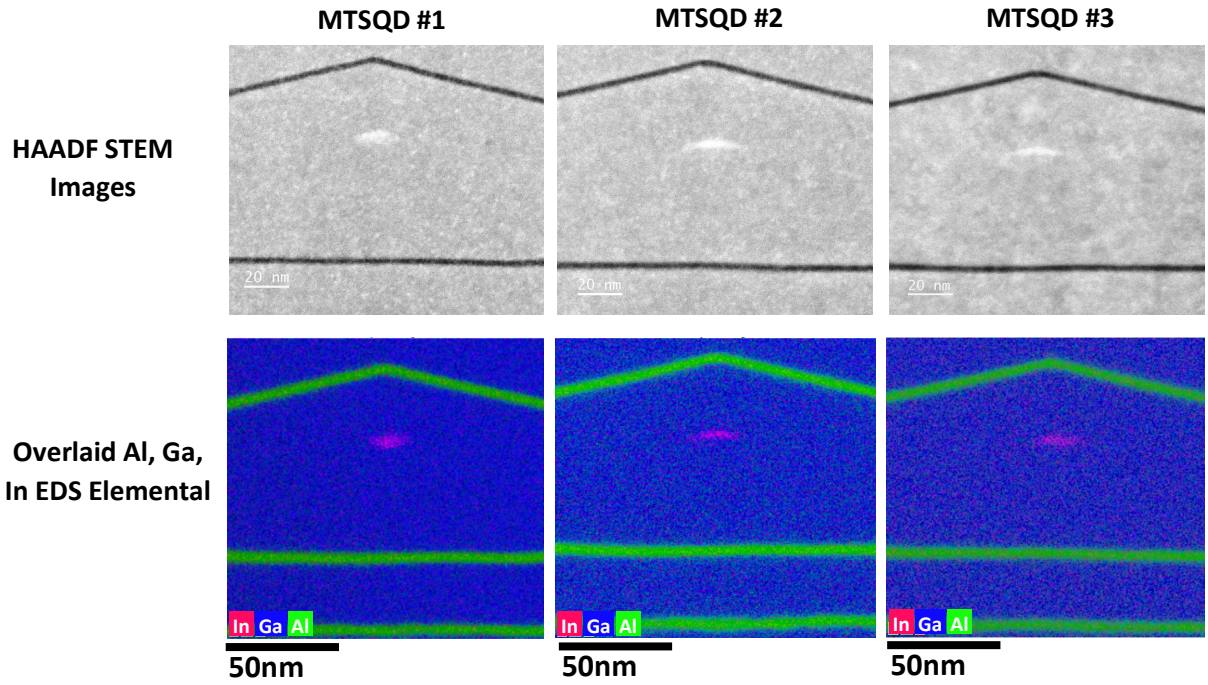

Fig.**7** Shows high-angle annular dark field image (upper panel) of the three consecutive MTSQDs in the array shown in Fig.6. The dark lines are AlAs marker layers placed periodically during growth to enable TEM to reveal the growth front evolution during SESRE. The light-shade region is the region of InGaAs QD formation while the grey region is the host material GaAs. The lower panel shows the energy dispersive spectroscopy (EDS) based elemental composition mapping of the single quantum dot region (In shown as violet), the GaAs region (Ga shown as blue), and the AlAs markers (Al shown as green). [Ref.9, To be published]

IV.5 Spectral Emission from Planarized (Buried) SQD Arrays

In Fig.8 we summarize the optical characteristics of the MTSQDs in 5X8 arrays for two samples of GaAs/InGaAs/GaAs SQDs: the upper set (panels a,b,c) shows the behavior of the *unplanarized* MTSQDs and serves as the reference for the lower set (panels d,e,f) showing the behavior of their counterpart that are buried under a *planarized* overlayer [6]. The annealing

attendant to the growth of the planarizing overlayer is, as expected, seen to cause a blue shift of ~15nm in the overall emission distribution and is accompanied by a *narrowing* of the emission nonuniformity to an unprecedented 2.8nm. We attribute this to interdiffusion of the In and Ga leading to an effectively lowered In content in the InGaAs region defining the effective quantum dot. The HBT coincidence count of two photon emission remains essentially the same, indicating single photon purity of ~99% is not affected by the planarizing overlayer growth.

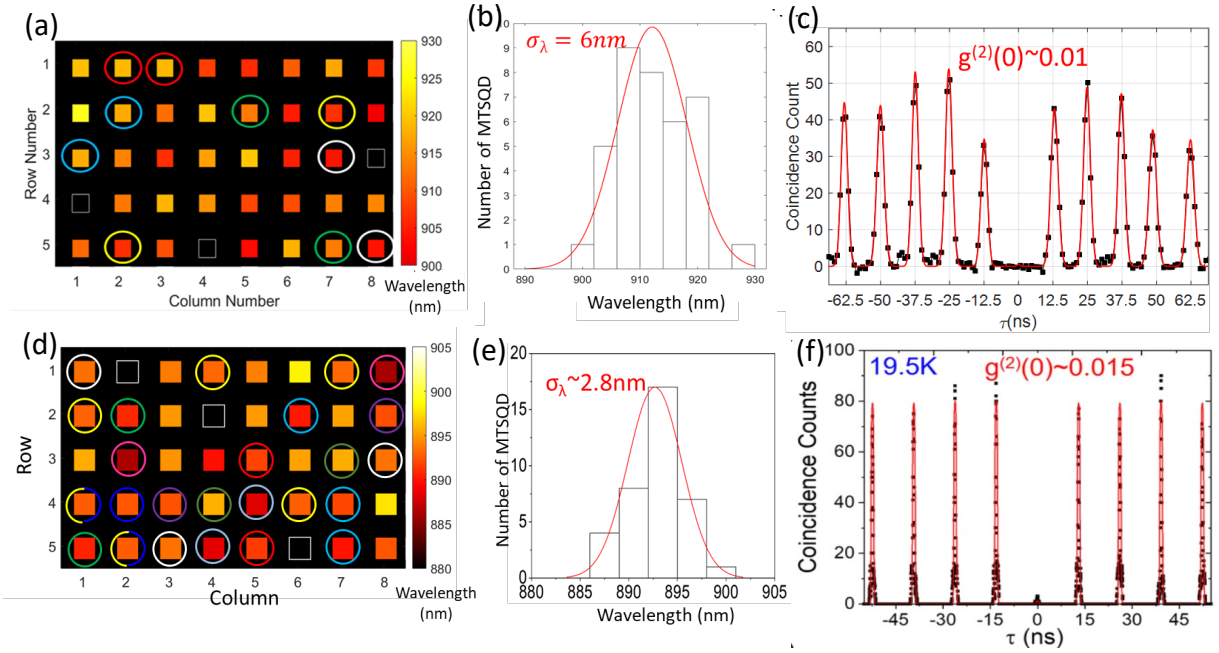

Fig. 8. Optical characteristics of the 5X8 array of 4.25ML $In_{0.5}Ga_{0.5}As$ MTSQDs: Upper and Lower rows are for *unplanarized* and *planarized* MTSQDs, respectively. Panels (a) and (d) show the emission wavelength distributions with the corresponding nonuniformity revealed in the histograms in panels (b) and (e), respectively. Like-color circles mark the MTSQDs that are emitting within the measurement resolution of 0.2nm. Note the shift of the average emission wavelength from ~912nm to ~892nm and the reduction in nonuniformity from ~6nm to ~2.8nm owing to the annealing experienced by the planarized array. Panels (c) and (f) show the HBT coincidence counts revealing a $g^{(2)}(0)$~ 0.01 (single photon purity ~99.5%) at ~12K and $g^{(2)}(0)$~ 0.015 (purity 99%) at 19.5K.

IV.6 Two-Photon Indistinguishability (Visibility): HOM Interferometry

Indistingushability of emitted photons is the essential characteristic of a quantum emitter for it to be of value to quantum informaiton processing. Traditionally this indistinguishability has been exracted from the HOM configuration to measure two photon interference. As briefly summrized below, we thus acquired the instrumentation for and carried out two-photon interference (TPI) measurements using HOM interferometer (Fig. 9).

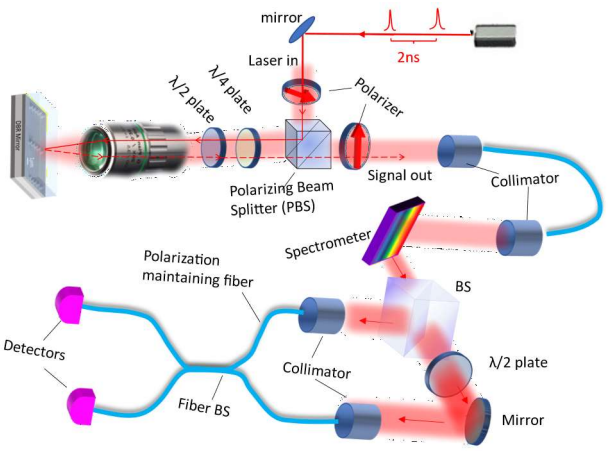

Fig 9. Schematic of Hong-Ou-Mandel interferometry for two photon interference visibility measurement using resonant excitation where scattered excitation laser is suppressed with a cross-polarization configuration with an extinction ratio $>1\times10^7$.

The indistinguishability of single photon emission from our MTSQD is measured using a Hong-Ou-Mandel (HOM) interferometer as schematically shown in Fig.9. We use a Ti-Sa laser to generate pairs of excitation pulses of width ~3ps with a time separation $\Delta t = 2\text{ns}$ to resonantly excite the MTSQD using cross polarization configuration microscope. The $\Delta t = 2\text{ns}$ time separation is determined by an unbalanced Michelson interferometer on the laser side. The excitation laser electric field is along [110] direction with an accuracy of $\pm3°$, and the photons emitted from MTSQD with polarization along $[\bar{1}10]$ direction (accuracy of $\pm3°$) are coupled into a polarization maintaining fiber. The quarter waveplate and half waveplate are used to compensate slight distortion from linear to elliptical polarization. A cross-polarized extinction ratio $>1\times10^7$ is achieved for the resonant excitation.

The single photons from MTSQD collected by the cross-polarization microscope are spectrally filtered by a 15ueV resolution spectrometer. Then the photons are guided to the first 50/50 beam splitter of the HOM interferometer and split into two branches. Photons in the two branches of the HOM interferometer are coupled to PM fibers using two collimators. The path length difference between these two branches is 2ns, matching with the excitation laser pulse time difference. Photons coupled into the PM fiber then interfere at the 50/50 fiber beam splitter and are detected by the superconducting nanowire detectors. One half wave plate is placed in one of the branches, enabling rotating the polarization of the photon in that branch with respect to the other. Photon detection events are registered using time-correlated single-photon counting (TCSPC) and time tagging electronics with a timing resolution ~50-100ps.

HOM Two-Photon Interferometry Results

Having established the MTSQD array emitted single photon purity >99% and nonuniformity as low as 1.8nm which is within the demonstrated technologies for local tuning to enable controlled interference between photons from distinct but known MTSQDs, the next important characteristic to be established is the indistinguishability between photons—from the same source and from different sources. For the latter, local tuning techniques need to be incorporated on-chip which was beyond the charter and scope of this grant. However, measuring the Hong-Ou-Mandel (HOM) two-photon indistinguishability (TPI), also dubbed *visibility*, for subsequent

photons emitted by the same source with controlled delay time (the typical visibility reported for quantum emitters in the literature) was within this grant's scope but required acquiring equipment to establish the HOM measurement facility. Fortunately, such equipment could be acquired via the DURIP and we set up the facility to carry out such measurements. The instrument response function for the HOM measurement is ~50-100ps.

For the HOM visibility measurements, MTSQD arrays were grown on GaAs substrates bearing an appropriately designed AlGaAs/GaAs DBR (distributed Bragg reflector) underneath to enhance the photon collection into the fiber (normal geometry) by an order of magnitude and thus makes the collection time for reliable signal to noise ration practical. The MTSQDs are resonantly excited with pulse of 3ps width and at Δt=2ns, the time interval between consecutively emitted photons. Figure 10 (a) shows the measured parallel polarization coincidence counts ($C_{\parallel}$) between the two output ports of the HOM interferometer as a function of the time difference (τ) between consecutive detection events in the co-polarized (parallel) configuration. The two photon interference is manifested in the strong reduction of the coincidence counts at τ=0 in the case of co-polarized configuration as compared to the data taken in the cross-polarized configuration (not shown).

The TPI visibility is extracted from the standard fomula $V = (C_{\perp} - C_{\parallel})/C_{\perp}$ with $C_{\perp}(C_{\parallel})$ being the total counts in the central peak at τ=0 with orthogonal (parallel) polarization. After correcting for the non-zero probability of double excitation of the QDs ($g^{(2)}(0) \sim 0.015$), the HOM parallel coincidence count data and the extracted visibility as a function of temperature are shown in Fig.**10**(a) and (b), respectively. It is to be noted that *no Purcell enhancement* of the spontaneous emission has been incorporated into the sample. Despite the lack of Purcell enhancement, the measured visibility of~82% at ~12.5K in the temperature range (>11K) accessible in our laboratory is **comparable to the best reported at these elevated temperatures**. With the resonant excitation cutting down on the spectral diffusion induced dephasing, the TPI visibility is largely limited by the phonon induced dephasing. Taking account of the typical known temperature dependence of the exciton dephasing time in the InGaAs/GaAs material system, the TPI visibility at 4K is expected to be >90% (Fig. **10**(b)). Thus, ***with the incorporation of a cavity with a modest Purcell enhancement of 3 to 5, the visibility can be pushed to the near 99% range***.

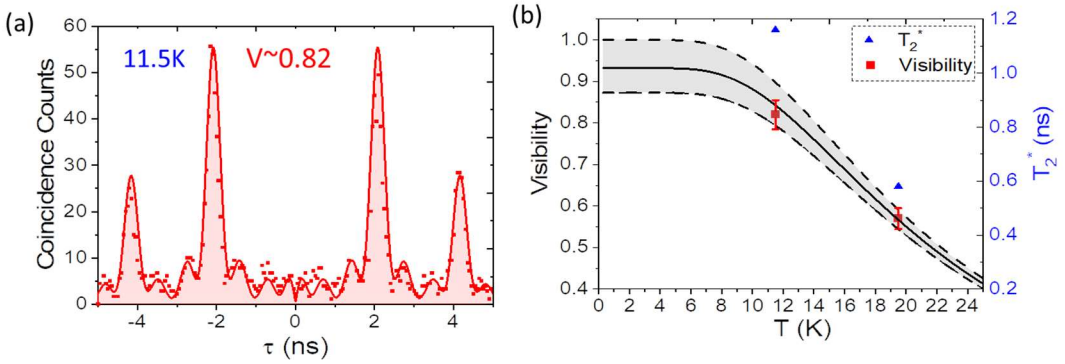

Fig.10. Panel (a) shows coincidence counts of TPI using HOM interferometry with the data collected under parallel polarization configuration with laser leak corrected. The MTSQD is excited by Ti:Sa laser at 780nm with two π/2 pulse pulses separated by 2ns and a repetition rate 78MHz. (b) Measured temperature dependent photon visibility (red sqaures) and dephasing time (blue triangles) of the measured MTSQD. The calculated TPI visibility as a function of temperatue is shown as black line. The grey region marks the range of TPI visibility as a function of temperature given the error range of the measured TPI visibility data at 19.5K.[From Ref.1]

Dephasing Time: A Three-Level System

The HOM coincidence count data (Fig. **10**), besides providing a value for the TPI visibility, also allows extracting a value for the dephasing time (T_2*) of the photons. In Fig.10, note the beating pattern occuring at ±0.6ns from the main peaks at τ=0, ±2ns and ±4ns in the measured HOM coincidence data. It shows that the emitted photon wavepacket is in a coherent superposition of the two states separated by 6.4μeV. This is independently confirmed by time-resolved PL data (not shown). The observed beat signal originates from single-photon self-interference, not two-photon interference. Barely any detected coincidence counts at τ=0 indicates that the *two-photon* interference (at τ=0) at the second beam splitter of the interferometer generates *energy-entangled photon pairs*. The probablity of a two-energy entangled photon pair generation decreases as one moves away from τ=0 as indicated by the observed rise of coincidence counts within τ~200ps.

To understand the intrisic physics, we used a three-level model to calculate the evolution of states. The HOM coincidence counts $g_{||}^{(2)}(\tau)$ and $g_{\perp}^{(2)}(\tau)$ can be respresented as,

$$g_{||}^{(2)}(\tau) = \int_0^{\infty} dt\, e^{-\frac{2t}{T_1}} \sin^2\left(\frac{\Delta}{2}t\right) \sin^2\left(\frac{\Delta}{2}(t+|\tau|)\right) \left[1 - e^{-\frac{2|\tau|}{T_2^*}}\right] e^{-\frac{|\tau|}{T_1}} \quad (1)$$

$$g_{\perp}^{(2)}(\tau) = \int_0^{\infty} dt\, e^{-\frac{2t}{T_1}} \sin^2\left(\frac{\Delta}{2}t\right) \sin^2\left(\frac{\Delta}{2}(t+|\tau|)\right) e^{-\frac{|\tau|}{T_1}} \quad (2)$$

We used Eq. 1 and 2 to analyze the measured data with the known decay lifetime T_1 and Δ obtained from the time-resolved PL data using Maximum Likelihood method to estimate the dephasing time T_2^*. The instrument response function was folded into the fitting as well. The fitting (red curve, Fig.10(a)) leads to **T_2^*~0.58ns**. Such a long dephasing time is also clearly seen in the *time-resolved* HOM coincidence counts plot shown in Fig.11 where the coincidence counts ($\propto g^{(2)}(t_1, t_1+\tau)$) corresponding to photon detection at time t_1 and $t_1+\tau$ at the two detectors are plotted as a funciton of t_1 and τ. The break at τ=0 and the rise of coindience counts with a scale of 200ps is clearly revealed in the measured data shown in Fig.11(a).

Simulation of the *Time Evolution* of HOM Indistinguishability

To further understand the HOM indistinguishability measurements above, we undertook studies of time evolution of the coincidence count in the HOM measuremenst. To this end, a fully quantum picture of the interference of two photon-wavepackets is employed. Each single photon wavepacket emitted from the SQD is modelled as a photon emitted from a 3-level system (reported in [1]), as

$$|\Psi_{Photon}(t)\rangle = \int_0^t f(t) a^{\dagger}(t)\, dt \text{ where } f(t) \propto \left(e^{-i\Delta t} e^{-\frac{t}{2T_1^{(a)}}} - e^{-\frac{t}{2T_1^{(b)}}}\right),$$

where Δ is the fine structure splitting between the two exciton states, and $T_1^{(a)/(b)}$ are the corresponding radiative decay life times. The time resolved HOM coincidence counts ($\propto g^{(2)}(t_1, t_1+\tau)$) corresponding to photon detection at time t_1 and $t_1+\tau$ at the two detectors is estimated as [1],

$$
\begin{aligned}
g^{(2)}(t_1, t_1+\tau) & \\
&= |f(t_1-\Delta T)f(t_1+\tau-2\Delta T)|^2 + |f(t_1+\tau-\Delta T)f(t_1-2\Delta T)|^2 \\
&+ |f(t_1)f(t_1+\tau-2\Delta T)|^2 + |f(t_1+\tau)f(t_1-2\Delta T)|^2 \\
&+ |f(t_1)f(t_1+\tau-\Delta T)|^2 + |f(t_1+\tau)f(t_1-\Delta T)|^2 \\
&+ 2|f(t_1-\Delta T)f(t_1+\tau-\Delta T)|^2 \left[1 - e^{-\frac{2|\tau|}{T_2^*}}\right] \qquad (3)
\end{aligned}
$$

The calculated response $g^{(2)}(t_1, t_1+\tau)$ using our three-level model and dephasing time T_2^* of 0.58ns is shown in Fig. 11(b). The calculation matches the measured data (Fig.11(a)) and thus supports the validity of the three level model of the MTSQD exciton and the dephasing time of $T_2^* \sim 0.58ns$. *Such a long dephasing time has, to the best of our knowledge, not been reported for SAQDs and appears to be unique to MTSQDs*.

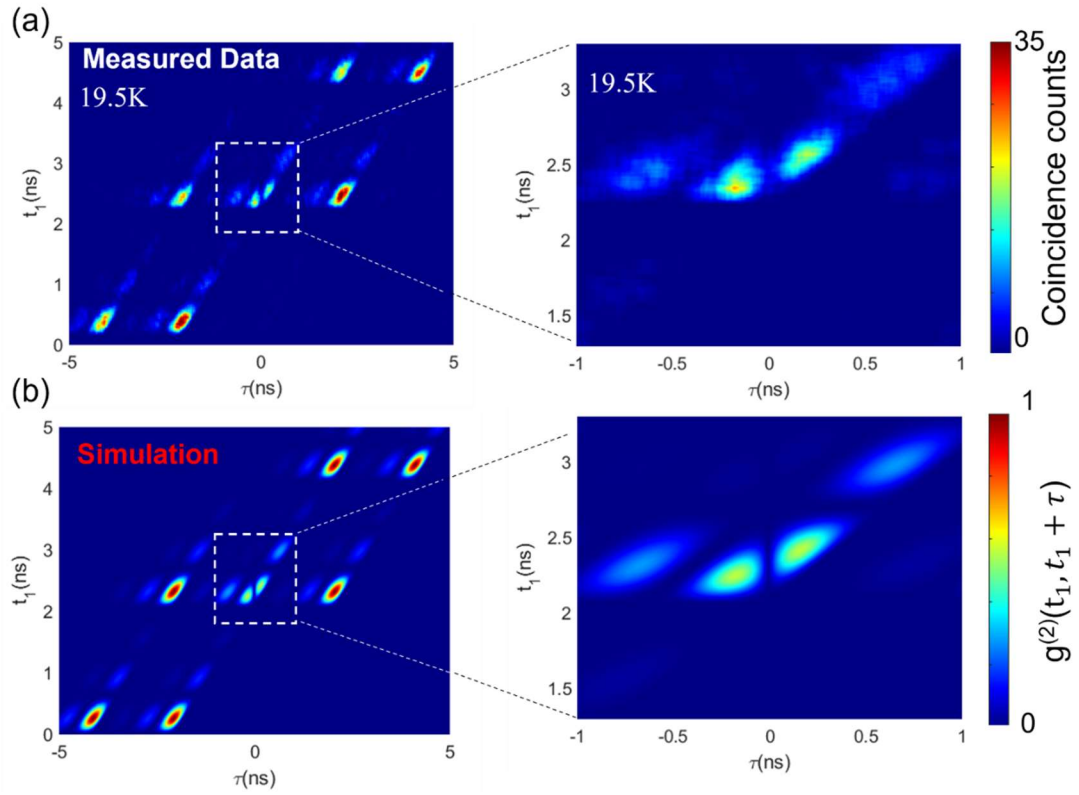

Fig.11 (a) Measured result of time-resolved HOM coincidence counts. The coincidence counts are plotted as a function of detector 1 detection time (t_1) and the time difference between detection event of the two detectors (τ). (b) Simulation result from the three-level model based on the known emission dynamics parameters. [From Ref.1]

IV.7 Scaling: Large Area MTSQD Array Growth and Imaging

The MTSQD characteristics discussed in the preceding sections were obtained through studies largely concentrated on 5X8 arrays with 5mm pitch distributed over a 1Cm radius area of the highest uniformity growth in our solid-source III-V MBE system (Riber 2300). We have

scaled up the array size to 50X50 with the 5mm pitch and distributed over the same 1Cm radius of the highest growth uniformity of the MBE system. Figure 12 below is an illustrative image of photoluminescence emission (panel (a)) from ~1200 MTSQDs sampled by the excitation beam from a 50X50 array containing 2500 MTSQDs. Panel (b) shows the emission spread histogram based upon measurements on a statistically-guided sample of 23 randomly selected MTSQDs.

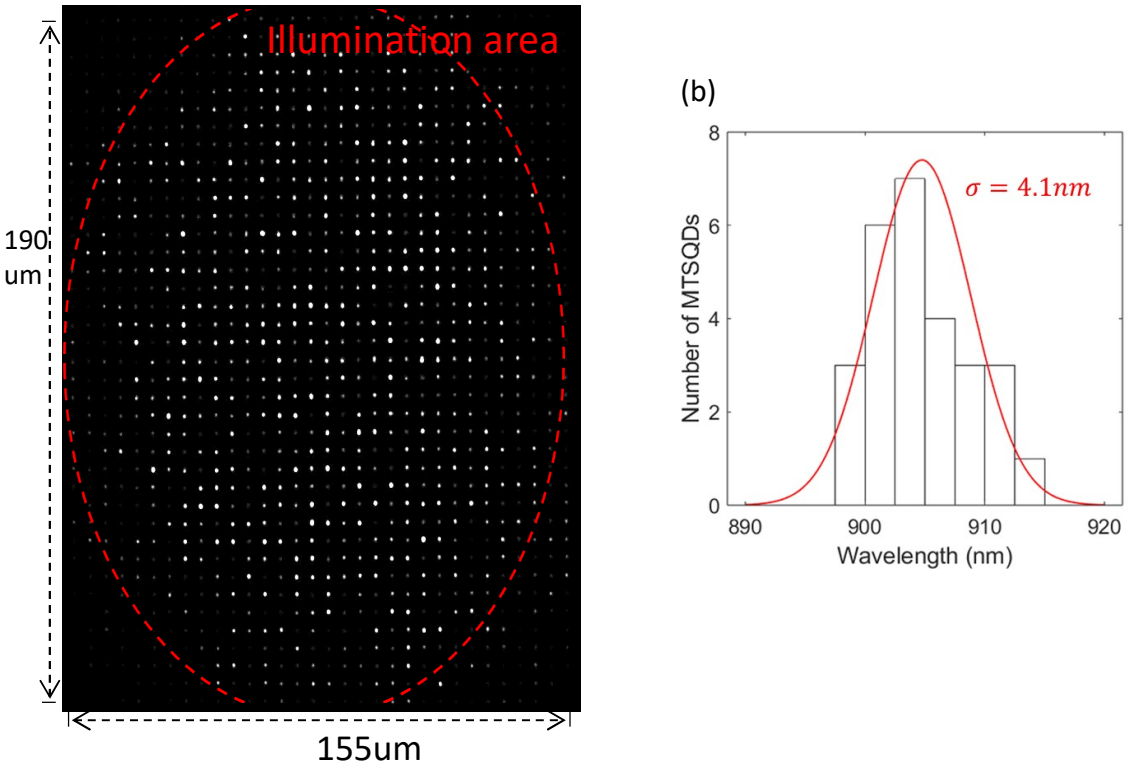

Fig 12. (a) Large area image of ~1250 planarized $In_{0.5}Ga_{0.5}As$ MTSQDs within the excitation beam area (red ellipse) in a 50 x 50 MTSQDs array. (b) histogram of the emission wavelength of 23 MTSQDs, revealing a uniformity σ_λ~4.1nm centered around 905nm. [Ref. 8, To be published]

Under a current AFOSR grant (FA9550-22-1--0376) we are implementing the instrumentation for large-area spectrally-resolved imaging that will enable a more robust statistical analysis.

Status of Optical Characteristics of MTSQDs in Spatially Ordered Arrays

GaAs/In0.5Ga0.5As/GaAs MTSQDs

- **Position control ΔR ≤ 5nm**
- **Spectral uniformity ~±4nm (for 2500 MTSQDs in 50 x 50 array)**
- **Quantum Efficiency ~100%**
- **Purity >99%**
- **Visibility ~0.82 (at 11.5K & *Without* Purcell Enhancement) -- (With Cavity at 4K, ~Unity)**

V. Outlook and Continuing Efforts

The accomplishment summed above is enabled by the *substrate-encoded size-reducing epitaxy* (SESRE) based synthesis of shape- and size-controlled mesa-top single quantum dots (MTSQDs) in scalable ordered arrays. Though implemented here in the GaAs/InGaAs/GaAs system, the SESRE approach based upon engineered surface stress gradients providing preferred direction for adatom migration is applicable to a variety of other material combinations including the InP and GaN based systems, covering the visible to telecommunication C-band and beyond.

Scalable quantum photonic circuits / networks require the following attributes: quantum emitters located at designed positions; amenable to horizontal photon emission and manipulation utilizing the mature 2D photonic crystal (PhC) technology; on-demand emission into appropriately matched PhC waveguide mode with near unity efficiency; having adequate spectral uniformity (i.e. nonuniformity within the range of demonstrated on-chip local tuning technologies); and possessing individual device-level requirements of simultaneously exhibiting near unity internal quantum efficiency, near unity purity per generation pulse, and near unity indistinguishability (visibility) for near unity photon detection probability per pulse. The demonstrated characteristics of the MTSQDs in arrays up to 50X50 are sufficiently close to these requirements and thus make a compelling case for studies of fabrication and testing the basic building blocks (Fig.13 (c)) of quantum photonic circuits around the demonstrated MTSQD arrays of sizes up to 50X50 and beyond.

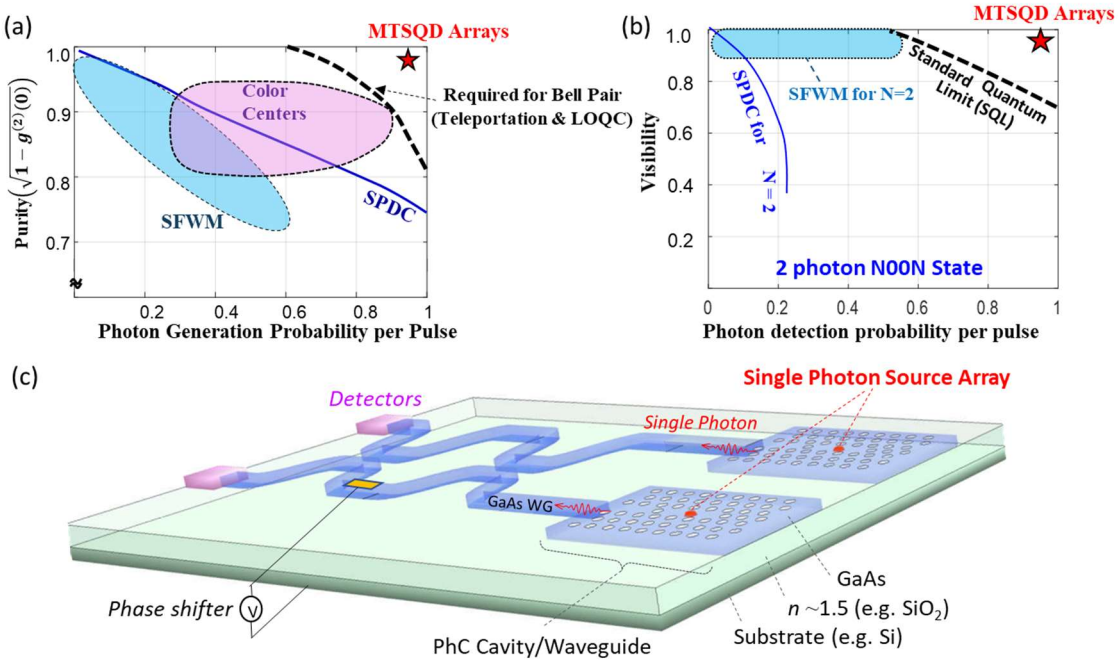

Fig.13 Potential of MTSQD Arrays for Quantum Optical Circuits. The requirements for (a) photon purity vs photon generation probability per pulse for single photon generation for creating linear optical quantum circuits and (b) the visibility vs photon detection probability per pulse of single photon sources for generation of 2 photon N00N states for quantum sensing at the standard quantum limit. Panel (c) is an illustration of an ordered MTSQD enabled on-chip Mach-Zehnder interferometer - the basic functional building block for on-chip quantum optical networks / circuits. [Taken from Ref. 1]

Our plans call for increasing the array size to 100X100 bearing 10,000 MTSQDs and beyond, establishing new approaches to large-area imaging and statistics-guided choice of sample size over which spectral characteristics (emission wavelength, photon purity, and visibility) with requisite resolution are measured. Needed are also developing methodologies for analyses of their behavior. We anticipate that approaches involving machine-learning and artificial intelligence will provide efficient ways of gathering statistically reliable data over not only the locally 10,000 MTSQDs but across such arrays distributed over 2Cm diameter area containing ~ 1 million MTSQDs.

In parallel, methodologies for hybrid integration of large arrays of these III-V based MTSQD quantum emitters with silicon photonics based emitted photon manipulation circuitry need to be developed beyond their feasibility demonstrations for systems with a handful of emitters chosen from a random distribution [2, 3]. We hope to contribute to such developments in collaboration with interested partners within the DoD research community as well as the larger community. Only through such partnership can one establish methodologies for rigorous assessment of a potentially viable platform for taking on-chip quantum photonics to the long-awaited next level—creation of well-designed functional quantum optical circuits (schematically shown in Fig. 13 c).

VI. References

1. J. Zhang, S. Chattaraj, Q. Huang, L. Jordao, S. Lu and A. Madhukar, "On-chip scalable highly pure and indistinguishable single-photon sources in ordered arrays: Path to quantum optical circuits", **Sci. Adv. 8, eabn9252 (2022).**

2, "Quantum Dots for Quantum Information Technologies", Ed. Peter Michler, (Springer **2017**). Thirteen chapters of this compilation, authored by the most active researchers, provide an exhaustive coverage of all aspects of epitaxial quantum dots and their potential for providing useful quantum photonic systems on a chip. The quantum dots covered are however largely the lattice-mismatch strain-driven defect-free 3D island quantum dots dubbed self-assembled quantum dots (SAQDs) that form at random locations and differing times, thereby acquiring differing size, shape, and composition resulting in highly inhomogeneous spectral emission (typically >40nm). The MTSQDs synthesized in spatially-regular arrays with well-controlled size and shape, remove both these deficiencies

3. Xiaoyan Zhou, Liang Zhai, and Jin Liu, "Epitaxial quantum dots: a semiconductor launchpad for photonic quantum technologies", **Photonics Insights, R07, vol.2 (2022**)

4. Jiefei Zhang, Swarnabha Chattaraj, Siyuan Lu and Anupam Madhukar, "Mesa-top quantum dot single photon emitter arrays: Growth, optical characteristics, and the simulated optical response of integrated dielectric nanoantenna-waveguide systems", **Jour. App. Phys., 120**. **243103 (2016)**

5. Jiefei Zhang, Swarnabha Chattaraj, Siyuan Lu and Anupam Madhukar, "Highly pure single photon emission from spectrally uniform surface-curvature directed mesa top single quantum dot ordered array", **Appl. Phys. Lett. 114**, **071102**, **(2019)**

6. J. Zhang, Q. Huang, S. Chattaraj, L. Jordao, S. Lu, and A. Madhukar, "Buried spatially-regular arrays of spectrally uniform single quantum dots as on-chip scalable single photon sources for quantum optical circuits", **APL Photonics**, **5**, **116106 (2020)**

7. S. Chattaraj, J. Zhang, S. Lu, and A. Madhukar, "On-Chip Integrated Single Photon Source Optically Resonant Metastructure Based Scalable Quantum Optical Circuits", **IEEE Jour. Quantum Electronics**, **56**, 1, **9300109 (2020)**.

8. Qi Huang, Siyuan Lu, Lucas Jordao, and Anupam Madhukar, "Large-area Spatially-Resolved Imaging of Emission from Mesa-top Single Quantum Dot Quantum Emitters in Ordered Arrays" To be published.

9. Lucas Jordao, Qi Huang, and Anupam Madhukar, "Scanning Transmission Electron Microscope studies of the Structure and Composition of GaAs/InGaAs Mesa-top Single Quantum Dots in Arrays", To be published.

.